Video Article

Sample Extraction and Simultaneous Chromatographic Quantitation of Doxorubicin and Mitomycin C Following Drug Combination Delivery in Nanoparticles to Tumor-bearing Mice

Rui Xue Zhang[1], Tian Zhang[1], King Chen[1], Ji Cheng[1], Paris Lai[1], Andrew M. Rauth[2], K. Sandy Pang[1], Xiao Yu Wu[1]

[1]Department of Pharmaceutical Sciences, University of Toronto

[2]Departments of Medical Biophysics and Radiation Oncology, University of Toronto, Ontario Cancer Institute, University Health Network

Correspondence to: Xiao Yu Wu at sxy.wu@utoronto.ca

URL: https://www.jove.com/video/56159
DOI: doi:10.3791/56159

Keywords: Cancer Research, Issue 128, HPLC, simultaneous analysis, biological sample extraction, combination chemotherapy, nanoparticles, pharmacokinetics, bio-distribution, doxorubicin, mitomycin C, doxorubicinol, blood, tumor

Date Published: 10/5/2017

Citation: Zhang, R.X., Zhang, T., Chen, K., Cheng, J., Lai, P., Rauth, A.M., Pang, K.S., Wu, X.Y. Sample Extraction and Simultaneous Chromatographic Quantitation of Doxorubicin and Mitomycin C Following Drug Combination Delivery in Nanoparticles to Tumor-bearing Mice. *J. Vis. Exp.* (128), e56159, doi:10.3791/56159 (2017).

Abstract

Combination chemotherapy is frequently used in the clinic for cancer treatment; however, associated adverse effects to normal tissue may limit its therapeutic benefit. Nanoparticle-based drug combination has been shown to mitigate the problems encountered by free drug combination therapy. Our previous studies have shown that the combination of two anticancer drugs, doxorubicin (DOX) and mitomycin C (MMC), produced a synergistic effect against both murine and human breast cancer cells *in vitro*. DOX and MMC co-loaded polymer-lipid hybrid nanoparticles (DMPLN) bypassed various efflux transporter pumps that confer multidrug resistance and demonstrated enhanced efficacy in breast tumor models. Compared to conventional solution forms, such superior efficacy of DMPLN was attributed to the synchronized pharmacokinetics of DOX and MMC and increased intracellular drug bioavailability within tumor cells enabled by the nanocarrier PLN.

To evaluate the pharmacokinetics and bio-distribution of co-administered DOX and MMC in both free solution and nanoparticle forms, a simple and efficient multi-drug analysis method using reverse-phase high performance liquid chromatography (HPLC) was developed. In contrast to previously reported methods that analyzed DOX or MMC individually in the plasma, this new HPLC method is able to simultaneously quantitate DOX, MMC and a major cardio-toxic DOX metabolite, doxorubicinol (DOXol), in various biological matrices (*e.g.,* whole blood, breast tumor, and heart). A dual fluorescent and ultraviolet absorbent probe 4-methylumbelliferone (4-MU) was used as an internal standard (I.S.) for one-step detection of multiple drug analysis with different detection wavelengths. This method was successfully applied to determine the concentrations of DOX and MMC delivered by both nanoparticle and solution approaches in whole blood and various tissues in an orthotopic breast tumor murine model. The analytical method presented is a useful tool for pre-clinical analysis of nanoparticle-based delivery of drug combinations.

Video Link

The video component of this article can be found at https://www.jove.com/video/56159/

Introduction

Chemotherapy is a primary treatment modality for many cancers yet it is often associated with severe adverse effects and limited efficacy due to drug resistance and other factors[1,2,3]. To improve the outcome of chemotherapy, drug combination regimens have been applied in the clinic based on considerations such as non-overlapping toxicities, different mechanisms of drug action, and non-cross drug resistance[4,5,6]. In clinical trials, a better tumor response rate was often observed using simultaneously administered drug combinations compared to a regimen of sequential drug delivery[7,8]. However, due to sub-optimal bio-distribution of free drug forms, simultaneous injection of multiple drugs can cause prominent normal tissue toxicity that outweighs the therapeutic effect[9,10,11]. Nanocarrier-based drug delivery has been shown to alter the pharmacokinetics and bio-distribution of encapsulated drugs, enhancing tumor-targeted accumulation[12,13,14]. As reviewed in our recent articles, nanoparticles co-loaded with synergistic drug combinations have demonstrated the capability to mitigate the problems encountered by free drug combinations, due to their controlled temporal and spatial co-delivery of multiple drugs to tumor tissue, enabling synergistic drug effects against cancer cells[4,15,16]. As a result, superior therapeutic efficacy and low toxicity have been demonstrated in both pre-clinical and clinical studies[4,17,18].

Our previous *in vitro* studies found that the combination of two anticancer drugs, doxorubicin (DOX) and mitomycin C (MMC), produced a synergistic effect against several breast cancer cells lines and, furthermore, co-loading DOX and MMC within polymer-lipid hybrid nanoparticles (DMPLN) overcame various multi-drug resistant associated efflux pumps (*e.g.,* P-glycoprotein and breast cancer resistant protein)[19,20,21]. *In vivo*, DMPLN enabled spatial-temporal co-delivery of DOX and MMC to tumor sites and increased bioavailability of drugs within cancer cells, as indicated by moderation of the formation of the DOX metabolite doxorubicinol (DOXol)[22]. As a result, the DMPLN enhanced tumor cell apoptosis, tumor growth inhibition, and prolonged host survival compared to free DOX and MMC combination or a liposomal DOX formulation[22,23,24,25].

Analyzing the actual amount of drugs co-delivered by a nanocarrier is critical for designing effective nanoparticle formulations. Many methods have been developed to analyze the plasma level of single DOX or MMC doses using high performance liquid chromatography (HPLC) alone or in combination with mass spectrometry (MS)[26,27,28,29,30,31,32,33,34]. However, these methods are often time-consuming and impractical for combination therapy as a large number of biological samples need to be prepared separately for analysis of multiple drugs (sometimes including drug metabolites). In addition to the strong plasma protein binding of DOX and MMC, red blood cells also have a great capacity to bind and concentrate many anticancer drugs[35,36]. Thus, plasma analysis for DOX or MMC may obfuscate actual blood drug concentrations. The present work (**Figure 1**) describes a simple and robust multiple drug analysis method using reverse phase HPLC to simultaneously extract and quantitate DOX, MMC and the DOX metabolite doxorubicinol (DOXol) from whole blood and various tissues (*e.g.,* tumors). It has been successfully applied to determine the pharmacokinetics and bio-distribution of DOX and MMC as well as the formation of DOXol after drug delivery via free solutions or nanoparticle forms (*i.e.*, DMPLN and liposomal DOX) in an orthotopically implanted murine breast-tumor mouse model after intravenous (i.v.) injection[22].

Protocol

All animal experiments were approved by the Animal Care Committee of University Health Network at the Ontario Cancer Institute and conducted in accordance with the Canadian Council on Animal Care Guidelines.

1. Biological Sample Preparation

1. **Collect the whole blood, major organs, and breast tumor at predetermined time-points after intravenous (i.v.) administration of drug-containing formulations (*e.g.*, DMPLN, liposomal DOX)**
    1. Inject a breast tumor-bearing mouse i.v. with a prepared drug-containing formulation.
    2. Anesthetize the mouse at designated time-points (*e.g.*, 15 min) by giving inhalable 2% isoflurane in a sealed chamber.
    3. Lay the anesthetized mouse on its back and put its nose through a nosepiece that constantly supplies 2% isoflurane.
    NOTE: To ensure the mouse undergoes deep anesthesia, gently pinch fore limbs of the mouse and look for any twitching movement.
    4. Thoroughly clean the chest and abdomen regions using 70% ethanol and then perform a terminal procedure of cardiac puncture on the deep anesthetized mice using a heparinized 1 mL syringe and a 23 G needle.
    5. Collect the whole blood into a labeled sodium heparin sprayed plastic tube and gently swirl the tube to ensure collected whole blood comes into contact with the coated heparin of the tube wall. Collect a minimum of 50 µL of whole blood. Always keep the samples on ice.
    6. Tape all four limbs of the mouse to secure it and open the abdominal cavity and ribcage of the mouse using a pair of scissors and forceps. Shift the intestines to the side and push the liver upward to sufficiently expose the portal vein. Cut the portal vein for the blood drainage.
    7. Perfuse the whole mouse body with 50 mL of ice-cold 0.9% saline through the heart using a 10 mL syringe with a 25 G needle.
    NOTE: Bend the needle at 90° for guiding the syringe into the portal vein.
    8. Excise organs in the following order: heart, lung, liver, spleen, kidneys. Then, separate the breast tumor from the surrounding connective tissues using a pair of incision scissors at the right mammary fat pad of the mouse. Collect all organs individually into 1.5 mL polypropylene tubes and quickly freeze them in liquid nitrogen.
    NOTE: Separate the gallbladder from the liver.
    9. Store the whole blood at 4 °C and excised tissues in the -80 °C freezer until later HPLC analysis.

2. **Extract DOX, MMC and DOXol from biological matrices.**
    1. Weigh all frozen dissected tissues quickly and transfer them into a 13 mL rounded-bottom conical tube. To avoid possible drug metabolism or degradation, keep the samples on ice.
    2. Add 1-5 mL of ice-cold cell lysis buffer into the tube.
    NOTE: The volume of buffer to use depends on the tissue weight based on the tissue-buffer ratio of 1 g: 5 mL (w/v); for small organs, such as heart and spleen, the ratio is 1 g: 2 mL.
    3. Use an up-down stroke motion to homogenize the tissue samples on ice at a speed of 18,000 rpm using an electric hand homogenizer.
    NOTE: Completed homogenization requires approximately 3 to 5 iterations of a short homogenization process of less than 15 s, followed by tissue cooling over ice between each short homogenization.
    4. Wash the 10 mm saw-tooth generator probe of the homogenizer with distilled deionized (DDI) H_2O, 70% ethanol, and then DDI H_2O between each tissue sample to avoid cross-contamination.
    5. Transfer 50 µL of tissue homogenate or whole blood into a 1.5 mL polypropylene micro-centrifuge tube and spike with 5 µL of an internal standard (I.S.) 4-methylumbelliferone (4-MU) (2000 ng/mL) into the tube.
    NOTE: 4-MU solution was prepared in methanol here.
    6. Add 250 µL of an ice-cold extraction solvent into the tube containing whole blood or tissue homogenate.
    NOTE: The extraction solvent consists of 60% acetonitrile (ACN) and 40% ammonium acetate (5 mM) with pH adjusted to pH = 3.5 using 0.05% formic acid. Use a 1:5 (v/v) sample: extraction solvent to volume ratio.
    7. Vigorously vortex the mixture for 2 min, centrifuge at 3,000 x g force at 4 ^{o}C for 10 min and pipet 200 µL supernatant into another pre-chilled fresh micro-centrifuge tube.
    8. Evaporate supernatant at 60 °C under a slow stream of nitrogen gas with protection from light.
    9. Reconstitute the dried residue with 100 µL of ice-cold methanol, vigorously vortex for 30 s and centrifuge at 3000 x g at 4 °C for another 5 min.
    10. Transfer the supernatant into a HPLC vial insert and place sample vials into an autosampler tray for injection.

2. HPLC Instrumentation and Operation Parameters

1. **Prepare HPLC mobile-phase with consistent reproducibility**
    1. Measure 500 mL of HPLC-grade H_2O using a graduated cylinder.
    2. Measure 500 mL of HPLC-grade acetonitrile (ACN) using a separate graduated cylinder.
    3. Carefully add 0.5 mL of trifluoroacetic acid (TFA) (CAUTION) into each of 500 mL of H_2O and ACN to obtain the mobile phase of H_2O and ACN containing 0.1% TFA, respectively.
       NOTE: TFA is corrosive and toxic and should be handled under a laboratory fume hood. All solvent mixtures are prepared at room temperature.
    4. Filter mobile phases through a nylon membrane filter with a 0.45 µm pore size and transfer it into clean HPLC reservoir bottles.

2. **Set-up HPLC instrumentation for simultaneous detection of DOX, MMC, and DOXol and I.S. 4-MU.**
    1. Switch on the gradient pump, de-gasser, auto-sampler, photodiode array detector, and multi λ fluorescence detector.
    2. Input the initial conditions of mobile-phase composition to 16.5% H_2O (0.1% TFA) and 83.5% ACN (0.1% TFA) (v/v).
    3. Set the UV detector on two channels, one at 310 nm for 4-MU (I.S.) and the other at 360 nm for MMC.
    4. Set the fluorescence detector on two channels, one at $\lambda_{ex}/\lambda_{em}$ =365/445 nm for 4-MU and the other at $\lambda_{ex}/\lambda_{em}$=480 nm/560 nm for DOX and DOXol, respectively.
    5. Set an isocratic flow rate of 1.0 mL/min.
    6. Equilibrate a preinstalled reverse phase C_{18} column (4.6 mm x 250 mm, 5 µm) at room temperature for 10 min for baseline establishment.

3. **Separate drugs (DOX, MMC, DOXol and 4-MU) using gradient mobile-phase condition.**
    1. Inject 15 µL of extracted and re-concentrated samples using the auto-sampler.
    2. Gradually change the initial mobile-phase condition (refer to protocol step 2.2.2) to 100% ACN (0.1% TFA) over 18 min using the automated gradient pump.
       NOTE: During the separation process, four channels (two UV absorbent and two fluorescent) appear simultaneously with each channel displaying one drug compound (refer to Protocol step 2.2.3 and 2.2.4).
    3. Maintain 100% of ACN (0.1% TFA) for 1 min and then return to the initial mobile phase condition within 1 min.
    4. Re-condition the column with the initial mobile phase at flow rate of 1.5 mL/min for 4 min for the next sample injection.

3. HPLC Validation

1. **Prepare working standards of DOX, MMC and DOXol, and 4-MU (I.S.).**
    1. Weigh separately 1 mg of DOX and MMC drug powder (CAUTION) and 4-MU on a fresh small weighing paper (3 x 3 $inches^2$).
       Note All anticancer drugs are considered a health hazard that can cause acute toxicity and germ cell mutagenicity on inhalation or ingestion. They should be handled carefully with gloves and masks.
    2. Transfer the weighed DOX, MMC and 4-MU into a new individual 1.5 mL polypropylene micro-centrifuge tube.
    3. Add 1 mL of methanol and vortex briefly to obtain 1 mg/mL concentration of DOX and MMC.
    4. Add 1 mL of methanol into a vial containing pre-weighed 1 mg of DOXol (CAUTION) and vortex briefly to obtain 1 mg/mL concentration of DOXol.
       NOTE: DOXol is a cardio-toxic metabolite and should be handled carefully.
    5. Pipette 20 µL of prepared stock solutions of DOX, MMC, DOXol and 4-MU into a new separate 1.5 mL polypropylene micro-centrifuge tube and add 980 µL of methanol to obtain a working standard of 20 µg/mL of each drug.
    6. Dilute 20 µg/mL of DOX, MMC and DOXol using methanol to obtain the working standards of 50 ng - 20 µg /mL for DOX, MMC, and DOXol and 2000 ng/mL for I.S. 4-MU.
    7. Seal the cap of the tube of working solutions with a narrow piece of paraffin film covering to prevent methanol evaporation, wrap the entire tube with aluminum foil to avoid exposure to direct light and store at -20 °C.

2. **Determine the linearity, precision, and accuracy of DOX, MMC and DOXol in biological matrices (*i.e.,* whole blood and tumor homogenate).**
    1. Simultaneously spike 5 µL of working standards of DOX and DOXol (50 ng/mL - 20 µg/mL), MMC (1,000 ng/mL - 16 µg/mL), and 4-MU (2 µg/mL) into 50 µL of blank whole blood or tissue homogenate in polypropylene micro-centrifuge tubes to obtain the standard concentration curve ranging from 5 - 2000 ng/mL for drug compounds and 200 ng/mL for 4-MU (I.S.).
    2. Perform the drug extraction assay described in Protocol 1.2.
    3. Use low, median and high concentrations of DOX and DOXol (50, 500, and 2,000 ng/mL) and MMC (100, 1000, 2,000 ng/mL) for intra- and inter-day precision and accuracy.
       NOTE: Prepare fresh standard concentrations on the day of analysis.

3. **Analysis of samples**
    1. Inject 15 µL of the sample using the auto-sampler.
    2. Gradually change the mobile phase over 0 to 18 min, increasing the composition of ACN over the interval.
    3. After 18 min, hold the mobile phase condition for 1 min.
    4. Return to the initial condition over the next 2 min, then re-equilibrate for 4 min before the next injection.
    5. After each sample run, note that the peaks of drug compounds with their retention time are shown as follow: MMC, DOXol, 4-MU (I.S.) and DOX.
    6. Integrate the peak area under curve (AUC) of drug compounds using HPLC software.
    7. Calculate the AUC ratio between individual drug compound and I.S. (Equation 1) and use the standard curves prepared under the same extraction procedures to determine the drug concentrations of DOX, MMC and DOXol in DMPLN formulation.

$$Peak\ Area\ Ratio = \frac{AUC_{drug}}{AUC_{I.S.}} \qquad Equation\ 1.$$

8. Calculate the drug recovery percentage (Equation 2) by comparing the drug concentrations reconstituted using methanol from the extracts of spiked biological samples to that of the standard ("neat") drug solution in methanol.

$$Drug\ Recovery\ \% = \frac{Peak\ Area\ Ratio_{extracted}}{Peak\ Area\ Ratio_{Neat}} \times 100 \qquad Equation\ 2.$$

Representative Results

Two anticancer drugs, DOX and MMC, as well as the DOX metabolite, DOXol, were simultaneously detected without any biological interference under the same applied gradient HPLC condition using 4-MU as the I.S. for both the fluorescence and UV detectors. DOX, MMC, DOXol and 4-MU were well-separated from each other with retention times of 5.7 min for MMC, 10.4 min for DOXol, 10.9 min for 4-MU, and 11.1 min for DOX (**Figure 2**). Each drug in whole blood and various tissues showed concentration linearity with correlation coefficients (R^2) ranging from 0.98 to 1.00 (**Figure 3** and **Table 1**). The lower limit of quantitation (LLOQ) of DOX, DOXol and MMC was 10 ng/mL, 10 ng/mL and 100 ng/mL in whole blood and 25 ng/mL, 25 ng/mL and 200 ng/mL in various tissues, respectively (**Table 1**). The HPLC method developed displayed less than 15% variation in terms of intra- and inter-day precision and accuracy for DOX, MMC and DOXol in whole blood and various biological matrices (*e.g.*, heart, lungs, liver, spleen, and kidneys), indicating excellent reproducibility (**Tables 2** and **3**). More than 85% of DOX and MMC was recovered from whole blood after extraction (**Table 4**).

The multidrug analysis procedures using one-step de-proteinization by an acidified extraction solvent followed by employing a multichannel HPLC method was successfully applied to determine the pharmacokinetics and bio-distribution of long-circulating or PEGylated nanoparticle-based drug delivery of both DOX alone or in combination with MMC in an orthotopic breast tumor murine model (**Figures 4** and **5**). **Figure 4** shows at least 6-fold higher drug concentrations in the blood over-time delivered by nanoparticles (*i.e.*, liposomal DOX and DMPLN) than the equivalent free drug solutions (*i.e.*, free DOX or free DOX-MMC) (**Figure 4**). Because of prolonged systemic circulation, nanoparticles were able to exploit the enhanced permeability and retention effects of the tumor, resulting in increased DOX and MMC accumulation in the breast tumor (**Figure 5A**)[37]. Meanwhile, the quantitatively determined formation of DOX metabolite DOXol in breast tumors over 24 h indicates a difference in drug bio-availability for various drug formulations (**Figure 5B**).

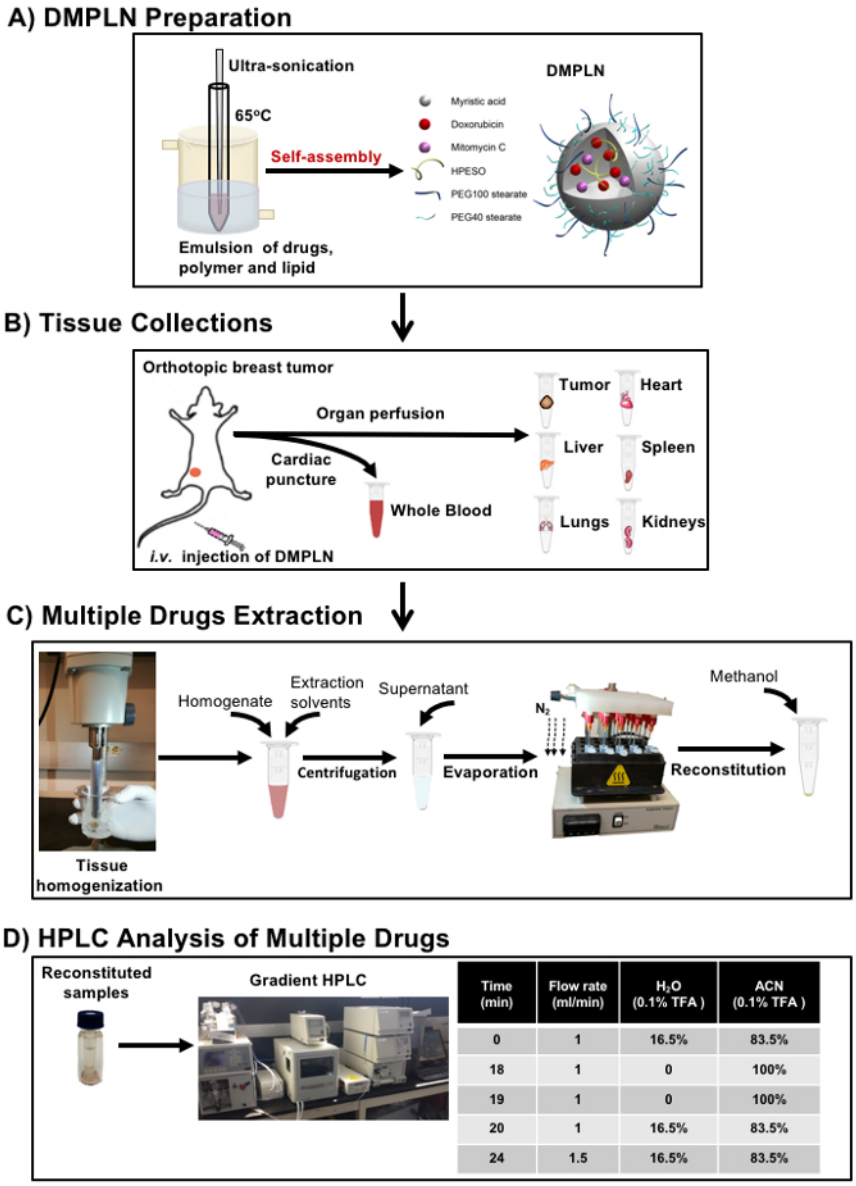

Figure 1: Illustration of the analysis processes for the simultaneous determination of DOX and MMC delivered by nanoparticles *in vivo*. (**A**) Preparation of DMPLN using a one-step ultra-sonication method followed by a self-assembly process; (**B**) Biological sample collections from an orthotopic breast tumor murine model; (**C**) Drug extraction from biological matrices and drug reconstitution; (**D**) Gradient HPLC for separation of DOX, MMC and DOXol. Please click here to view a larger version of this figure.

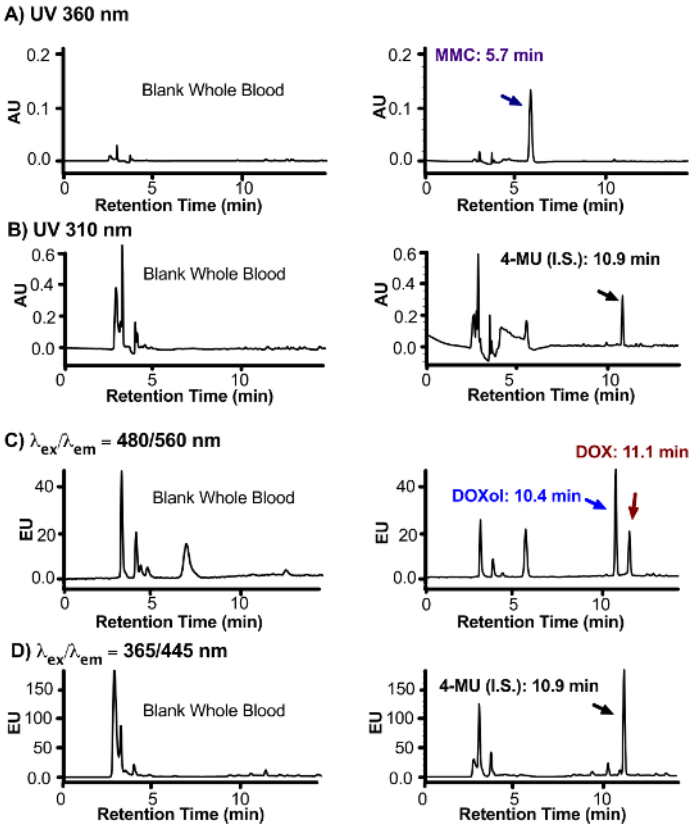

Figure 2: Comparison of chromatograms of blank whole blood and drug mixtures in blood. Comparison of chromatograms of blank whole blood and drug mixtures in blood using HPLC coupled to UV and fluorescence detectors at (**A**) UV 360 nm for MMC; (**B**) UV 310 nm for I.S. 4-MU; (**C**) Fluorescence at $\lambda_{ex/em}$ = 480/560 nm for DOX and DOXol; (**D**) Fluorescence at $\lambda_{ex/em}$ = 365/445 nm for I.S. 4-MU. AU is absorbance unit and EU is fluorescence unit. The injected concentrations of MMC, DOX, and DOXol and their I.S. 4-MU were 100 ng/mL, 50 ng/mL, 50 ng/mL and 200 ng/mL, respectively. Please click here to view a larger version of this figure.

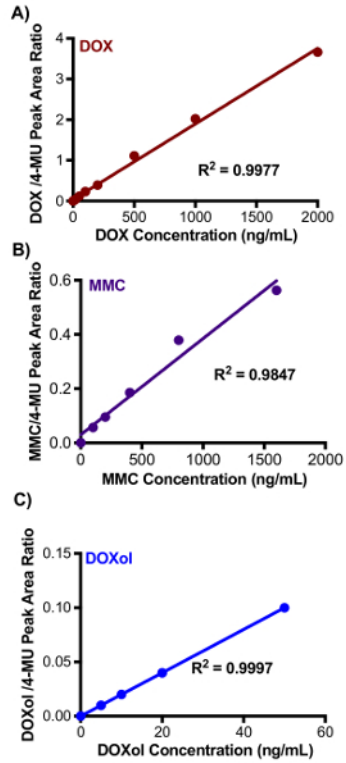

Figure 3: Representation of standard curves for MMC, DOX and DOXol in whole blood. The concentration ranges were from 100 ng/mL to 2000 ng/mL for MMC (**A**), from 5 ng/mL to 2000 ng/mL for low DOX concentration (**B**), and from 5 ng/mL to 50 ng/mL for DOXol (**C**). Please click here to view a larger version of this figure.

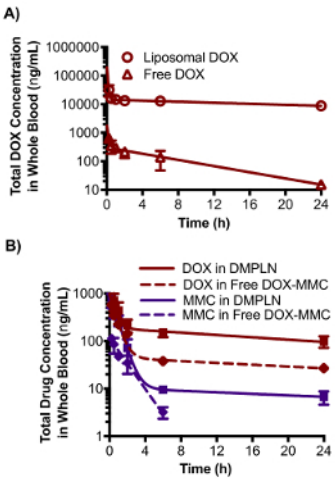

Figure 4: Application of the multiple drug analysis system, using a multichannel and gradient HPLC method, to study the pharmacokinetics of long-circulating nanoparticle-based drug delivery. (**A**) Time-blood concentration profiles of DOX in mono-therapy using free drug solutions (free DOX) or a liposomal formulation (see **Table of Materials**); (**B**) Time-blood concentration profiles of DOX and MMC as a free drug combination (free DOX-MMC) or DMPLN. Whole blood was collected at various time points up to 24 h after a single *i.v.* injection to mice bearing an orthotopic murine breast tumor. All mice were treated with 9.2 mg/kg DOX alone or in combination with 2.9 mg/kg MMC. Because the LLOD of MMC was 100 ng/mL using the HPLC coupled UV detector, MMC concentration after 6 h post-injection was determined by mass spectrometry. The figure has been modified from Zhang *et al*. Nanomedicine with permission[22]. All the data points are presented as mean ± standard deviation (SD) with n = 3. Please click here to view a larger version of this figure.

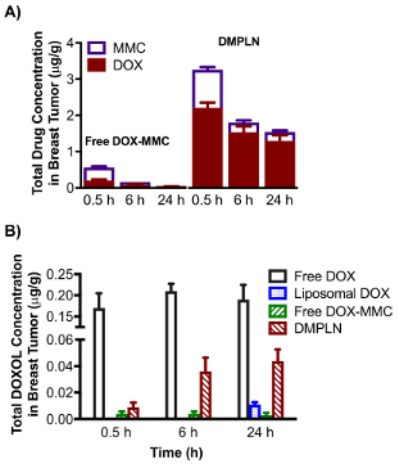

Figure 5: Application of multiple drug analysis using the gradient HPLC method to study the tumor bio-distribution of a nanoparticle-based drug delivery system. (**A**) Total DOX and MMC concentrations of free DOX-MMC or DMPLN in breast tumors; (**B**) Total DOXol metabolite formation in breast tumors treated with mono- or combination DOX chemotherapy. All mice were treated with 9.2 mg/kg DOX alone or in combination with 2.9 mg/kg MMC. Because free DOX-MMC had a low tumor accumulation that was out of LLOD of MMC using the HPLC coupled UV detector, MMC concentration in free DOX-MMC was determined by mass spectrometry. The figure has been modified from Zhang *et al*. Nanomedicine with permission[22]. All the data points are presented as mean ± SD with n = 3. Please click here to view a larger version of this figure.

Biological Matrices	R^2			LLOQ (ng/ml)		
	DOX	DOXol	MMC	DOX	DOXol	MMC
Whole Blood	0.9905±0.0242	0.9946±0.0068	0.9907±0.0103	10	10	100
Breast Tumour	0.9992±0.0059	0.9973±0.0021	0.9995±0.0103	25	25	200
Liver	0.9957±0.0085	0.9961±0.0038	0.9987±0.0007	25	25	200
Heart	0.9969±0.0080	0.9994±0.0005	0.9990±0.0014	25	25	200
Spleen	0.9903±0.0003	0.9992±0.0002	1.0000±0.0002	25	25	200
Kidneys	0.9915±0.0040	0.9993±0.0002	0.9902±0.0003	25	25	200
Lungs	0.9932±0.0217	0.9994±0.0010	0.9994±0.0007	25	25	200

Table 1: Linearity and LLOQ of DOX, MMC and DOXol in various biological matrices. The data represent mean ± SD for n = 3.

A)

Anticancer Drug	DOX in Whole Blood			
	Intra-day		Inter-day	
Concentration (ng/ml)	Precision%	Accuracy%	Precision%	Accuracy%
50	4.6	95.0	4.0	90.9
500	2.1	102.4	13.9	114.0
2000	0.7	100.1	3.8	97.2

B)

Anticancer Drug	MMC in Whole blood			
	Intra-day		Inter-day	
Concentration (ng/ml)	Precision%	Accuracy%	Precision%	Accuracy%
100	4.9	97.4	7.4	95.4
1000	1.4	98.4	2.2	98.2
2000	2.6	97.0	2.3	100.8

C)

Drug Metabolite	DOXol in Whole blood			
	Intra-day		Inter-day	
Concentration (ng/ml)	Precision%	Accuracy%	Precision%	Accuracy%
50	1.4	99.2	1.9	89.1
500	0.8	100.0	7.7	103.4
2000	1.2	101.3	0.9	101.8

Table 2: Intra- and inter-day precision and accuracy of DOX, MMC and DOXol in mouse whole blood (n = 3).

A)

DOX	Intra-day											
	Liver		Heart		Spleen		Kidney		Lung		Breast Tumor	
Concentration (ng/mL)	Precision%	Accuracy%	Precision%	Accuracy%	Precision%	Accuracy%	Precision%	Accuracy%	Precision%	Accuracy%	Precision%	Accuracy%
50	3.7	97.3	3.4	99.7	5.3	94.4	9.6	95.6	14.1	90.8	9.6	95.6
500	1.4	101.4	0.2	104.4	5.0	100.9	6.6	93.7	0.8	99.1	6.6	93.7
2000	3.7	104.1	0.0	102.3	5.0	104.6	2.9	98.8	0.1	98.0	2.9	98.8
DOX	Inter-day											
	Liver		Heart		Spleen		Kidney		Lung		Breast Tumor	
Concentration (ng/mL)	Precision%	Accuracy%	Precision%	Accuracy%	Precision%	Accuracy%	Precision%	Accuracy%	Precision%	Accuracy%	Precision%	Accuracy%
50	1.2	90.9	3.1	101.9	4.2	91.0	10.7	110.9	4.0	95.4	10.7	110.8
500	4.2	98.1	0.4	100.2	0.1	93.4	4.0	101.8	3.0	103.3	4.0	101.8
2000	6.9	101.6	2.0	99.9	0.4	92.9	3.0	103.3	5.1	107.9	3.0	103.3

B)

MMC	Intra-day											
	Liver		Heart		Spleen		Kidney		Lung		Breast Tumor	
Concentration (ng/mL)	Precision%	Accuracy%	Precision%	Accuracy%	Precision%	Accuracy%	Precision%	Accuracy%	Precision%	Accuracy%	Precision%	Accuracy%
100	13.7	120.1	12.9	93.6	0.6	98.1	20.9	108.7	4.5	100.8	10.9	108.7
1000	1.7	103.2	3.8	104.6	2.3	96.1	1.6	99.8	3.6	97.1	1.6	99.8
2000	3.4	97.8	2.8	89.6	2.5	97.2	2.7	97.9	3.7	96.3	2.7	98.0
MMC	Inter-day											
	Liver		Heart		Spleen		Kidney		Lung		Breast Tumor	
Concentration (ng/mL)	Precision%	Accuracy%	Precision%	Accuracy%	Precision%	Accuracy%	Precision%	Accuracy%	Precision%	Accuracy%	Precision%	Accuracy%
100	14.9	110.9	14.1	90.5	1.2	100.8	14.8	87.7	2.7	93.8	14.8	87.7
1000	1.3	101.4	2.9	98.4	2.7	100.7	5.1	92.9	2.9	91.2	5.1	92.9
2000	0.8	99.6	2.4	98.4	2.4	100.3	3.0	92.6	4.4	88.9	3.0	92.6

C)

DOXol	Intra-day											
	Liver		Heart		Spleen		Kidney		Lung		Breast Tumor	
Concentration (ng/mL)	Precision%	Accuracy%	Precision%	Accuracy%	Precision%	Accuracy%	Precision%	Accuracy%	Precision%	Accuracy%	Precision%	Accuracy%
50	6.0	106.5	3.9	102.6	0.9	104.5	3.2	96.2	1.1	99.0	3.2	96.2
500	7.5	108.8	2.4	101.6	0.8	97.4	0.9	98.9	0.6	99.3	0.9	99.0
2000	5.5	106.2	2.3	102.1	0.6	103.4	1.2	98.8	0.8	97.0	1.2	98.8
DOXol	Inter-day											
	Liver		Heart		Spleen		Kidney		Lung		Breast Tumor	
Concentration (ng/mL)	Precision%	Accuracy%	Precision%	Accuracy%	Precision%	Accuracy%	Precision%	Accuracy%	Precision%	Accuracy%	Precision%	Accuracy%
50	4.7	111.3	3.2	101.6	2.7	98.2	2.3	97.8	3.1	96.3	2.3	97.8
500	3.6	109.2	2.0	101.1	1.6	98.9	1.6	98.2	2.2	97.4	1.6	98.2
2000	1.9	100.1	2.1	101.4	2.0	98.7	2.0	97.8	2.0	98.5	2.0	97.8

Table 3: Intra- and inter-day precision and accuracy of DOX, MMC and DOXol in breast tumors (n = 3).

	Recovery % from Whole Blood	
Theoretical Concentration (ng/ml)	DOX	MMC
50	94.5 ± 14	93.5 ± 24
500	85.2 ± 9	95.4 ± 7
1000	88.4 ± 6	88.5 ± 7

Table 4: DOX and MMC recovery percentage in the whole blood samples after extraction (n = 3). The data represents mean ± SD for n = 3.

Discussion

Compared to other chromatographic methods that enable the detection of a single drug species at a time, the present HPLC protocol is able to simultaneously quantitate three drug compounds (DOX, MMC, and DOXol) in the same biological matrix without the need to change the mobile phase. This preparation and analysis method has been successfully applied to determine the pharmacokinetics and bio-distribution of two nanoparticle-based drug delivery systems (*i.e.,* liposomal DOX and DMPLN)[22]. Since the *PEGylated* nanoparticles prolong systemic circulation of loaded drug resulting in high blood drug concentrations over a long period of time (>24 h), the described chromatographic method is cost-effective for large scale sample analysis of nanoparticle co-loaded drug combinations in pre-clinical studies[22]. The pharmacokinetics of free DOX solution and liposomal DOX shown in **Figure 4A** is consistent with reported literature data in rodents[38,39], further supporting the validity of the current method. Although the UV photodiode-array detector allows multiple-channels to simultaneously detect and display drugs using variable wavelengths (*i.e.,* 310 nm for 4-MU and 360 nm for MMC), the intrinsic detection limit of UV detector is less sensitive than the fluorescence detector. Thus, for fast eliminating, non-fluorescent drugs like MMC delivered in free solutions, the drug concentrations at later time points may fall below the LLOQ of UV detector.

In general, a short chromatography column (*e.g.*, 5 cm) would be used for HPLC analysis to minimize the elution time and operating time. Yet, in the case of analyzing multiple drug compounds, especially those with very similar molecular structures (*e.g.*, DOX and its metabolite DOXol), it is difficult to achieve full separation using the short column due to intrinsic column efficiency. Thus, both a longer column (*e.g.*, 25 cm, used in the current protocol) and an optimization of HPLC parameters during the development of the method are needed to achieve a good peak resolution. Although DOX, DOXol and 4-MU were eluted at close retention time, the interference between DOX/DOXol and 4-MU was not observed in the prepared sample concentration (*e.g.*, 50 ng/mL) in the chromatographs (**Figure 2**). However, a high DOX concentration (*e.g.*, ~10,000 ng/mL) delivered by nanoparticles as a result of long blood circulation time could interfere with the peak detection of itself and other compounds (*e.g.*, DOXol) and may result in self-quenching of DOX fluorescence[40,41]. In this case, a proper sample dilution using blank whole blood may be required before sample analysis to determine drug concentrations.

Extraction methods can further complicate the analysis of chemotherapeutic drug combinations. Although DOX or MMC can be extracted using various extraction methods, including solid phase extraction (SPE) or liquid-solid extraction, these procedures are time-consuming and expensive. Some of the extraction methods result in poor recovery and possible drug degradation when hydrochloric acid is added to the extraction solvent[42,43,44]. For large scale biological sample preparations, the present extraction method is simple, quick and only requires the addition of small amounts of non-hazardous organic solvent for efficient de-proteinization followed by systematic sample reconstitution using methanol. High recovery rates (>85%) were achieved for all drug samples of varying concentrations by systematically applying the same extraction protocol. Although variability still exists, the differences are statistically insignificant. To further reduce the variation, the optimization of individual sample extraction at low and high drug concentrations may be required. Note that the extraction method used does not distinguish free released drug from drug remaining in the nanoparticle as nanoparticles were completely dissolved after addition of organic solvents. Thus, the true pharmacokinetics of nanoparticles alone *vs.* free drug alone requires the development of a numerical deconvolution method using mathematical modelling to predict their behavior *in vivo*[45].

In summary, a simple and selective HPLC method was developed for simultaneous determination of DOX, MMC and Doxol *in vivo*. The present method shows robustness, selectivity, precision and accuracy over a broad range of drug concentrations for the mouse whole blood and tissues. This method has been successfully applied to obtain the blood concentration-time profile of DOX and MMC and the bio-distribution of DOX, DOXol and MMC in breast tumors and other major organs (*e.g.,* heart). This protocol provides a useful tool for elucidating macro- and microscopic *in vivo* mechanisms of nanoparticle-delivered DOX containing drug combination chemotherapy.

Disclosures

The authors have no competing financial interests and conflicts of interest.

Acknowledgements

The authors gratefully acknowledge the equipment grant from the Natural Science and Engineering Research (NSERC) Council of Canada for HPLC, the operating grant from the Canadian Institute of Health Research (CIHR) and Canadian Breast Cancer Research (CBCR) Alliance to X.Y. Wu, and the University of Toronto Scholarship to R.X. Zhang and T. Zhang.

References

1. Holohan, C., Van Schaeybroeck, S., Longley, D. B., & Johnston, P. G. Cancer Drug Resistance: An Evolving Paradigm. *Nat. Rev. Cancer.* **13** (10), 714-726 (2013).
2. Szakacs, G., Paterson, J. K., Ludwig, J. A., Booth-Genthe, C., & Gottesman, M. M. Targeting Multidrug Resistance in Cancer. *Nat. Rev. Drug. Discov.* **5** (3), 219-234 (2006).
3. Kong, A.-N. T. *Inflammation, Oxidative Stress, and Cancer: Dietary Approaches for Cancer Prevention.*Kong, A.N.T., ed., CRC Press, Florida, USA (2013).
4. Zhang, R. X., Wong, H. L., Xue, H. Y., Eoh, J. Y., & Wu, X. Y. Nanomedicine of Synergistic Drug Combinations for Cancer Therapy - Strategies and Perspectives. *J. Control. Release.* **240** 489-503 (2016).
5. Webster, R. M. Combination Therapies in Oncology. *Nat. Rev. Drug. Discov.* **15** (2), 81-82 (2016).
6. Waterhouse, D. N., Gelmon, K. A., Klasa, R., Chi, K., Huntsman, D., Ramsay, E., Wasan, E., Edwards, L., Tucker, C., Zastre, J., Wang, Y. Z., Yapp, D., Dragowska, W., Dunn, S., Dedhar, S., & Bally, M. B. Development and Assessment of Conventional and Targeted Drug Combinations for Use in the Treatment of Aggressive Breast Cancers. *Curr. Cancer. Drug. Targets.* **6** (6), 455-489 (2006).
7. Cancello, G., Bagnardi, V., Sangalli, C., Montagna, E., Dellapasqua, S., Sporchia, A., Iorfida, M., Viale, G., Barberis, M., Veronesi, P., Luini, A., Intra, M., Goldhirsch, A., & Colleoni, M. Phase Ii Study with Epirubicin, Cisplatin, and Infusional Fluorouracil Followed by Weekly Paclitaxel with Metronomic Cyclophosphamide as a Preoperative Treatment of Triple-Negative Breast Cancer. *Clin. Breast. Cancer.* **15** (4), 259-265 (2015).
8. Masuda, N., Higaki, K., Takano, T., Matsunami, N., Morimoto, T., Ohtani, S., Mizutani, M., Miyamoto, T., Kuroi, K., Ohno, S., Morita, S., & Toi, M. A Phase Ii Study of Metronomic Paclitaxel/Cyclophosphamide/Capecitabine Followed by 5-Fluorouracil/Epirubicin/Cyclophosphamide as Preoperative Chemotherapy for Triple-Negative or Low Hormone Receptor Expressing/Her2-Negative Primary Breast Cancer. *Cancer. Chemother. Pharmacol.* **74** (2), 229-238 (2014).
9. Carrick, S., Parker, S., Thornton, C. E., Ghersi, D., Simes, J., & Wilcken, N. Single Agent Versus Combination Chemotherapy for Metastatic Breast Cancer. *Cochrane. Database. Syst. Rev.* **15** (2), CD003372 (2009).
10. Cardoso, F., Bedard, P. L., Winer, E. P., Pagani, O., Senkus-Konefka, E., Fallowfield, L. J., Kyriakides, S., Costa, A., Cufer, T., Albain, K. S., & Force, E.-M. T. International Guidelines for Management of Metastatic Breast Cancer: Combination Vs Sequential Single-Agent Chemotherapy. *J. Natl. Cancer. Inst.* **101** (17), 1174-1181 (2009).
11. Alba, E., Martin, M., Ramos, M., Adrover, E., Balil, A., Jara, C., Barnadas, A., Fernandez-Aramburo, A., Sanchez-Rovira, P., Amenedo, M., Casado, A., & Spanish Breast Cancer Research, G. Multicenter Randomized Trial Comparing Sequential with Concomitant Administration of Doxorubicin and Docetaxel as First-Line Treatment of Metastatic Breast Cancer: A Spanish Breast Cancer Research Group (Geicam-9903) Phase Iii Study. *J. Clin. Oncol.* **22** (13), 2587-2593 (2004).
12. Sadat, S. M., Saeidnia, S., Nazarali, A. J., & Haddadi, A. Nano-Pharmaceutical Formulations for Targeted Drug Delivery against Her2 in Breast Cancer. *Curr. Cancer Drug Targets.* **15** (1), 71-86 (2015).
13. Devadasu, V. R., Wadsworth, R. M., & Ravi Kumar, M. N. V. Tissue Localization of Nanoparticles Is Altered Due to Hypoxia Resulting in Poor Efficacy of Curcumin Nanoparticles in Pulmonary Hypertension. *Eur. J. Pharm. Biopharm.* **80** (3), 578-584 (2012).
14. Li, S. D., & Huang, L. Pharmacokinetics and Biodistribution of Nanoparticles. *Mol. Pharm.* **5** (4), 496-504 (2008).
15. Zhang, R. X., Ahmed, T., Li, L. Y., Li, J., Abbasi, A. Z., & Wu, X. Y. Design of Nanocarriers for Nanoscale Drug Delivery to Enhance Cancer Treatment Using Hybrid Polymer and Lipid Building Blocks. *Nanoscale.* **9** (4), 1334-1355 (2017).
16. Wang, X., Li, S., Shi, Y., Chuan, X., Li, J., Zhong, T., Zhang, H., Dai, W., He, B., & Zhang, Q. The Development of Site-Specific Drug Delivery Nanocarriers Based on Receptor Mediation. *J. Control. Release.* **193** 139-153 (2014).
17. Batist, G., Gelmon, K. A., Chi, K. N., Miller, W. H., Jr., Chia, S. K., Mayer, L. D., Swenson, C. E., Janoff, A. S., & Louie, A. C. Safety, Pharmacokinetics, and Efficacy of Cpx-1 Liposome Injection in Patients with Advanced Solid Tumors. *Clin. Cancer Res.* **15** (2), 692-700 (2009).
18. Mayer, L. D., Harasym, T. O., Tardi, P. G., Harasym, N. L., Shew, C. R., Johnstone, S. A., Ramsay, E. C., Bally, M. B., & Janoff, A. S. Ratiometric Dosing of Anticancer Drug Combinations: Controlling Drug Ratios after Systemic Administration Regulates Therapeutic Activity in Tumor-Bearing Mice. *Mol. Cancer Ther.* **5** (7), 1854-1863 (2006).
19. Prasad, P., Cheng, J., Shuhendler, A., Rauth, A. M., & Wu, X. Y. A Novel Nanoparticle Formulation Overcomes Multiple Types of Membrane Efflux Pumps in Human Breast Cancer Cells. *Drug Deliv. Transl. Res.* **2** (2), 95-105 (2012).
20. Shuhendler, A. J., Cheung, R. Y., Manias, J., Connor, A., Rauth, A. M., & Wu, X. Y. A Novel Doxorubicin-Mitomycin C Co-Encapsulated Nanoparticle Formulation Exhibits Anti-Cancer Synergy in Multidrug Resistant Human Breast Cancer Cells. *Breast Cancer Res. Treat.* **119** (2), 255-269 (2010).

21. Shuhendler, A. J., O'Brien, P. J., Rauth, A. M., & Wu, X. Y. On the Synergistic Effect of Doxorubicin and Mitomycin C against Breast Cancer Cells. *Drug Metabol. Drug Interact.* **22** (4), 201-233 (2007).
22. Zhang, R. X., Cai, P., Zhang, T., Chen, K., Li, J., Cheng, J., Pang, K. S., Adissu, H. A., Rauth, A. M., & Wu, X. Y. Polymer-Lipid Hybrid Nanoparticles Synchronize Pharmacokinetics of Co-Encapsulated Doxorubicin-Mitomycin C and Enable Their Spatiotemporal Co-Delivery and Local Bioavailability in Breast Tumor. *Nanomedicine.* **12** (5), 1279-1290 (2016).
23. Zhang, T., Prasad, P., Cai, P., He, C., Shan, D., Rauth, A. M., & Wu, X. Y. Dual-Targeted Hybrid Nanoparticles of Synergistic Drugs for Treating Lung Metastases of Triple Negative Breast Cancer in Mice. *Acta. Pharmacol. Sin.* 1-13 (2017).
24. Shuhendler, A. J., Prasad, P., Zhang, R. X., Amini, M. A., Sun, M., Liu, P. P., Bristow, R. G., Rauth, A. M., & Wu, X. Y. Synergistic Nanoparticulate Drug Combination Overcomes Multidrug Resistance, Increases Efficacy, and Reduces Cardiotoxicity in a Nonimmunocompromised Breast Tumor Model. *Mol. Pharm.* **11** (8), 2659-2674 (2014).
25. Prasad, P., Shuhendler, A., Cai, P., Rauth, A. M., & Wu, X. Y. Doxorubicin and Mitomycin C Co-Loaded Polymer-Lipid Hybrid Nanoparticles Inhibit Growth of Sensitive and Multidrug Resistant Human Mammary Tumor Xenografts. *Cancer. Lett.* **334** (2), 263-273 (2013).
26. Rafiei, P., Michel, D., & Haddadi, A. Application of a Rapid Esi-Ms/Ms Method for Quantitative Analysis of Docetaxel in Polymeric Matrices of Plga and Plga-Peg Nanoparticles through Direct Injection to Mass Spectrometer. *Am. J. Anal. Chem.* **6** (2), 164-175 (2015).
27. Daeihamed, M., Haeri, A., & Dadashzadeh, S. A Simple and Sensitive Hplc Method for Fluorescence Quantitation of Doxorubicin in Micro-Volume Plasma: Applications to Pharmacokinetic Studies in Rats. *Iran. J. Pharm. Res.* **14** (Suppl), 33-42 (2015).
28. Alhareth, K., Vauthier, C., Gueutin, C., Ponchel, G., & Moussa, F. Hplc Quantification of Doxorubicin in Plasma and Tissues of Rats Treated with Doxorubicin Loaded Poly(Alkylcyanoacrylate) Nanoparticles. *J. Chromatogr. B Analyt. Technol. Biomed. Life Sci.* **887-888**, 128-132 (2012).
29. Al-Abd, A. M., Kim, N. H., Song, S. C., Lee, S. J., & Kuh, H. J. A Simple Hplc Method for Doxorubicin in Plasma and Tissues of Nude Mice. *Arch Pharm Res.* **32** (4), 605-611 (2009).
30. Loadman, P. M., & Calabrese, C. R. Separation Methods for Anthraquinone Related Anti-Cancer Drugs. *J. Chromatogr. B Biomed. Sci. Appl.* **764** (1-2), 193-206 (2001).
31. Zhang, Z. D., Guetens, G., De Boeck, G., Van Cauwenberghe, K., Maes, R. A., Ardiet, C., van Oosterom, A. T., Highley, M., de Bruijn, E. A., & Tjaden, U. R. Simultaneous Determination of the Peptide-Mitomycin Kw-2149 and Its Metabolites in Plasma by High-Performance Liquid Chromatography. *J. Chromatogr. B Biomed. Sci. Appl.* **739** (2), 281-289 (2000).
32. Alvarez-Cedron, L., Sayalero, M. L., & Lanao, J. M. High-Performance Liquid Chromatographic Validated Assay of Doxorubicin in Rat Plasma and Tissues. *J. Chromatogr. B Biomed. Sci. Appl.* **721** (2), 271-278 (1999).
33. Paroni, R., Arcelloni, C., De Vecchi, E., Fermo, I., Mauri, D., & Colombo, R. Plasma Mitomycin C Concentrations Determined by Hplc Coupled to Solid-Phase Extraction. *Clin. Chem.* **43** (4), 615-618 (1997).
34. Song, D., & Au, J. L. Direct Injection Isocratic High-Performance Liquid Chromatographic Analysis of Mitomycin C in Plasma. *J Chromatogr B Biomed Appl.* **676** (1), 165-168 (1996).
35. Schrijvers, D. Role of Red Blood Cells in Pharmacokinetics of Chemotherapeutic Agents. *Clin. Pharmacokinet.* **42** (9), 779-791 (2003).
36. Colombo, T., Broggini, M., Garattini, S., & Donelli, M. G. Differential Adriamycin Distribution to Blood Components. *Eur. J. Drug Metab. Pharmacokinet.* **6** (2), 115-122 (1981).
37. Maeda, H., Nakamura, H., & Fang, J. The Epr Effect for Macromolecular Drug Delivery to Solid Tumors: Improvement of Tumor Uptake, Lowering of Systemic Toxicity, and Distinct Tumor Imaging in Vivo. *Adv. Drug Deliv. Rev.* **65** (1), 71-79 (2013).
38. Gustafson, D. L., Rastatter, J. C., Colombo, T., & Long, M. E. Doxorubicin Pharmacokinetics: Macromolecule Binding, Metabolism, and Excretion in the Context of a Physiologic Model. *J. Pharm. Sci.* **91** (6), 1488-1501 (2002).
39. Gabizon, A., Shiota, R., & Papahadjopoulos, D. Pharmacokinetics and Tissue Distribution of Doxorubicin Encapsulated in Stable Liposomes with Long Circulation Times. *J. Natl. Cancer Inst.* **81** (19), 1484-1488 (1989).
40. Motlagh, N. S., Parvin, P., Ghasemi, F., & Atyabi, F. Fluorescence Properties of Several Chemotherapy Drugs: Doxorubicin, Paclitaxel and Bleomycin. *Biomed. Opt. Express.* **7** (6), 2400-2406 (2016).
41. Mohan, P., & Rapoport, N. Doxorubicin as a Molecular Nanotheranostic Agent: Effect of Doxorubicin Encapsulation in Micelles or Nanoemulsions on the Ultrasound-Mediated Intracellular Delivery and Nuclear Trafficking. *Mol. Pharm.* **7** (6), 1959-1973 (2010).
42. Cielecka-Piontek, J., Jelińska, A., Zając, M., Sobczak, M., Bartold, A., & Oszczapowicz, I. A Comparison of the Stability of Doxorubicin and Daunorubicin in Solid State. *J. Pharm. Biomed Anal.* **50** (4), 576-579 (2009).
43. Gilbert, C. M., McGeary, R. P., Filippich, L. J., Norris, R. L. G., & Charles, B. G. Simultaneous Liquid Chromatographic Determination of Doxorubicin and Its Major Metabolite Doxorubicinol in Parrot Plasma. *J. chromatogr. B Analyt. Technol. Biomed. Life sci.* **826** (1-2), 273-276 (2005).
44. Liu, Z. S., Li, Y. M., Jiang, S. X., & Chen, L. R. Direct Injection Analysis of Mitomycin C in Biological Fluids by Multidemension High Performance Liquid Chromatography with a Micellar Mobile Phase.*J. Liq. Chromatogr. Relat. Technol.* **19** (8), 1255-1265 (1996).
45. Zhou, Y., He, C., Chen, K., Ni, J., Cai, Y., Guo, X., & Wu, X. Y. A New Method for Evaluating Actual Drug Release Kinetics of Nanoparticles inside Dialysis Devices Via Numerical Deconvolution. *J. Control. Release.* **243**, 11-20 (2016).

